Collapse of masonry arches in Romanesque and Gothic constructions

D. Aita and F. Foce
Dipartimento di Scienze per l'Architettura, Università di Genova, Italy

R. Barsotti and S. Bennati
Dipartimento di Ingegneria Strutturale, Università di Pisa, Italy

ABSTRACT: Round and ogival (or pointed) arches are found bearing the weight of the vertical walls in many vaulted masonry structures, especially architectural designs typical of the Romanesque and Gothic periods. It would therefore appear interesting to examine such arch-wall systems and attempt to determine the stress levels as a function of the relevant geometrical and mechanical parameters and assess their safety margin with respect to conditions of incipient collapse, as well as the actual mechanism by which such collapse would occur. A simplified version of the problem can be studied by following two different approaches, which are in fact complementary to each other. The first, which is based on a proper extension of Durand-Claye's method of the stability area, aims at determining the set of statically admissible solutions within the limits imposed by the material's ultimate compressive and tensile strengths and the limited shear capacity of the joints. When such area shrinks to a point, a limit equilibrium condition is attained in the arch-wall system. The second approach instead studies the stress and strain fields generated in the arch, which is considered to be made of material offering poor resistance to tension and whose mechanical behaviour can be modelled, as a first approximation, via a non-linear elastic constitutive relation. In this case, the problem is addressed by studying and numerically integrating systems of non-linear equations. The condition of incipient collapse is considered to be reached when the residual stiffness of the system falls below a predetermined fraction of its initial value. As will be shown, the two approaches, rather than offering two alternative paths, actually provide two complementary views of the same problem.

1 INTRODUCTION

The structural response of masonry arches and vaults has been studied extensively over the past three centuries and still represents a topical issue in modern structural mechanics research. By looking at the historical development of the theories of the masonry arch, two alternative theoretical approaches, corresponding to what we now call 'limit' and 'elastic' analysis, may be identified.

The first approach focuses on the stability of the entire masonry structure, conceived of as composed of rigid voussoirs subject to unilateral constraints and friction at the joints. This is the equilibrium approach followed in the first 18th century studies on masonry arches and subsequently developed during the early 19th century on the basis of Coulomb's renowned method of maxima and minima. When equilibrium of such an assemblage is impossible, the voussoirs undergo some relative displacements, which transform the arch into a mechanism. Some of the authors have recently extended a method proposed by the French scholar Durand-Claye in 1867 (see Foce et al. [2003]) to the case of masonry arches made up of materials characterized by bounded compressive strength.

The second approach aims instead to determine the stress and strain fields within the masonry arch. This approach involves the complete set of the equilibrium, compatibility and stress-

strain equations and, because of the strong material non-linearity, computationally demanding numerical analysis are frequently required for their solution (Alfano, et al. [2000], Lourenço [2005]). Taking up the groundbreaking work of Signorini, some of the authors (Bennati et al. [2001]) have proposed to model the masonry arch as a non-linear elastic curved beam. Within this framework, collapse is conventionally attained when the residual stiffness of the arch becomes less than a preset fraction of its initial value.

The alternative between limit and elastic structural approaches - *stability* versus *non-linear elastic solution* - is not so radical as it may seem at first sight. Indeed the two methods of analysis may be fruitfully applied in conjunction. To this aim, this paper presents a parallel treatment of masonry arches in terms of both non-linear elastic analysis and Durand-Claye's method. The two procedures have been applied to two different arch types of great import in Romanesque and Gothic constructions from both the mechanical and architectonic perspectives: the semicircular and the pointed arch. The purpose is to compare the different bearing capacities of semicircular and pointed arches loaded by their self-weight and by the weight of a superimposed wall, thereby evaluating the maximum wall height compatible with equilibrium of the system and the strength of the masonry.

2 EQUILIBRIUM OF THE ARCH-WALL SYSTEM

In this paper we consider the equilibrium problem of semicircular and pointed masonry arches subject to their own weight and to the weight of a superimposed wall (Figure 1).

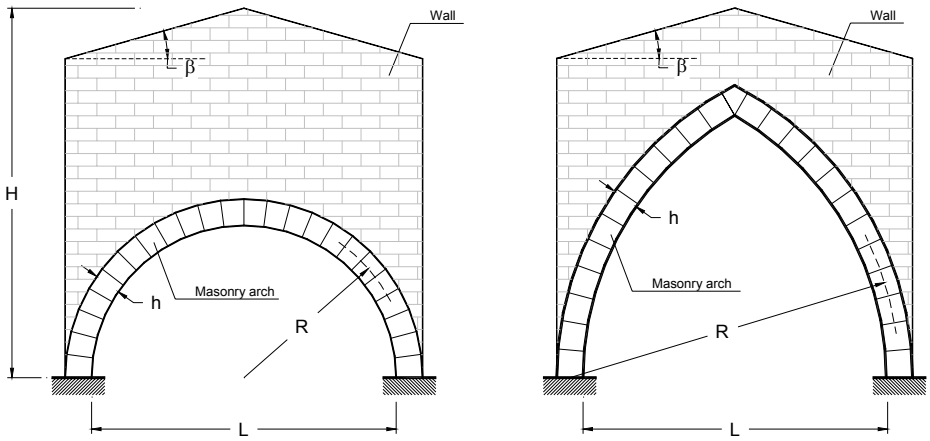

Figure 1. Scheme of the arch-wall system for semicircular (left) and pointed (right) arches.

In order to compare the load-bearing capacities of arches characterized by different shapes, in all the cases we will assume a clear arch span L = 10 m, a compressive strength σ_c = 20 MPa, a tensile strength σ_t = 0 and a Young modulus E = 4 GPa; all other geometrical parameters will be left free.

With the aim of investigating the effects on the solution produced by variations in the shapes of both the arch and the wall, we will consider different values for the arch's thickness, h, and for the angle β formed between the extrados of the wall and the horizontal direction. Both circular and pointed arches are assumed to have horizontal springings; the radius of the line of axis is $R = (L + h)/2$ for circular arches and $R = L + h$ for pointed arches.

For each value of β we will determine the maximum height of the wall compatible with the load-bearing capacity of the arch, the stress and strain distributions, the cracking pattern within the arch and the displacement field for different values of the arch thickness h by studying both the progressive reduction of the stability area and the evolution of the non-linear elastic solution. In all cases *the superimposed wall is treated as a dead vertical load acting on the masonry*

arch.

It is worth noting that the 'limit condition' assumes a different meaning depending on whether we adopt the 'stability area' method or non-linear elastic analysis: according to the first, it corresponds to the attainment of a 'limit equilibrium' state, while in the second, it is related to the vanishing of the arch residual stiffness or, alternatively, to a 'limit displacement' condition.

3 THE SOLUTION METHODS

3.1 The stability area method

Durand-Claye's method is a graphical procedure to define the so-called *area of stability* at the crown section of a symmetrical arch, that is to say, the area within which the extremes of the vectors representing the crown thrust must be included in order that both the global equilibrium of the structure and the limited strength of masonry be respected.

Here we provide only a brief qualitative description of the method; further details can be found in some previous works (Foce et al. [2003], Aita et al. [2004]), which present an extensions of Durand-Claye's original methods in order to account for any tensile and compressive strength.

According to this procedure, we consider a symmetric masonry arch with finite compressive and tensile strength σ_c and σ_t. By taking into account the limit bending moment and the shear force that may be transmitted through any joint along the arch, it is possible to determine the maximum and minimum values of the thrust P at the crown section for each value of the eccentricity e of its application point with respect to the centroid of the cross-section. By scanning every joint of the arch and every eccentricity e, the set of all admissible thrust values may be found; the locus of the extremes of the vectors representing such forces constitutes the so-called *area of stability* (Figure 2). When this area shrinks to a point, the limit condition is attained, and a unique admissible thrust line exists.

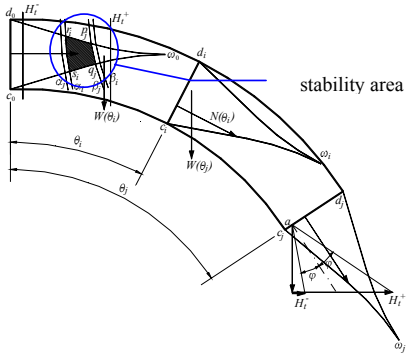

Figure 2. The stability area.

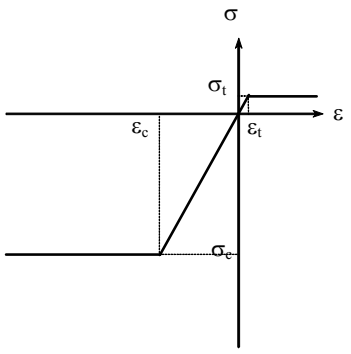

Figure 3. Non-linear stress-strain relation.

3.2 Non-linear elastic analysis

The alternative approach makes use of a simple one-dimensional non-linear elastic model, which relies on the piecewise-linear constitutive relation between longitudinal strains and stresses plotted in figure 3, where σ_t and σ_c are the material's tensile and compressive strength, respectively. Under the assumption commonly accepted in the theory of the bending of beams, namely that any given cross-section remains plane and orthogonal to the line of axis after bending, a non-linear constitutive relation able to roughly describe the complex mechanical behaviour of masonry may be established between the axial strain ε_0 and cross-sectional curvature χ, on the one hand, and the axial force N and bending moment M, on the other.

Due to the assumed bounded tensile and compressive strengths, the set of all internal force values compatible with the assumed constitutive relation is a closed bounded domain in the (*N*, *M*) plane (figure 4).

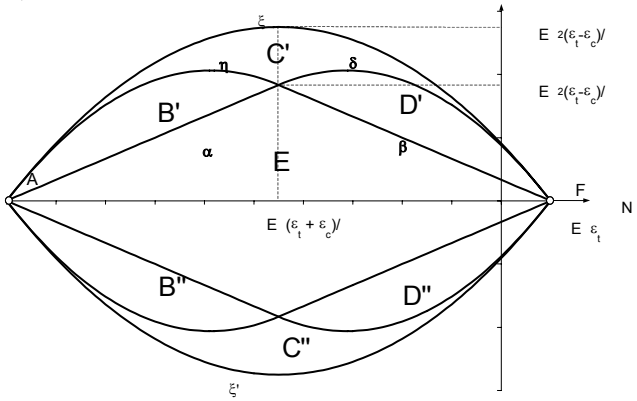

Figure 4. The elastic domain.

Different analytic expressions for the constitutive relation hold in the different regions into which the domain is subdivided. By way of example, in region *C'* (where the stress distribution is non-linear under both tension and compression), it is

$$\begin{cases} N = \dfrac{E}{8\chi}[(\varepsilon_c - \varepsilon_t)(\varepsilon_t + \varepsilon_c - 2\varepsilon_0) + h\chi(\varepsilon_c + \varepsilon_t)], \\ M = \dfrac{E(\varepsilon_c - \varepsilon_t)}{24\chi^2}[(\varepsilon_c - \varepsilon_t)^2 + 3(\varepsilon_t + \varepsilon_c - 2\varepsilon_0)^2 - 3h^2\chi^2]. \end{cases} \tag{1}$$

Analogous relations, omitted here for the sake of brevity, hold in the other regions.

Simple calculations show that under the foregoing hypotheses, and in the case of a circular arch with radius *R*, the tangential displacement component *u* may be expressed as

$$u(\theta) = A + B\sin(\theta) + C\cos(\theta) + \int_{\theta_0}^{\theta}[1-\cos(t-\theta)][-R^2\chi(t) + R\varepsilon_0''(t)]dt\,, \tag{2}$$

where θ is the angle formed between the radial direction and the horizontal at any point along the line of the arch axis, *A*, *B* and *C* are three constants, and the primes denote differentiation with respect to θ. Moreover, analogous expressions hold for the radial displacement component *v,* as well as the rotation φ, as $v = u' - R\varepsilon_0$, and $\varphi = (u + v')/R$.

Under general load and constraint conditions, equation (2) and the analogous ones for *v* and φ lead to a non-linear set of equations in the three constants *A*, *B* and *C* and the redundant end-reaction components. Due to the strong non-linearity of the problem, the solution to this set of equations can be obtained in closed form only for cases of relatively simple loads and geometries. In general, the solution is sought via an iterative method. For the present context, an *ad hoc* numerical procedure has been used, following a modified standard Newton-Raphson scheme. The arch's behaviour is assumed to be linear during any given iteration. In this way, we obtain a linear set of equations, which is solved by performing the required integration numerically. The curvature and axial strain are updated, and the procedure is then repeated until the difference between the values of the internal forces *N* and *M* furnished by the constitutive relations and the corresponding ones calculated from the equilibrium equations becomes lower than a small fixed threshold value (for more details see Bennati, 2007).

4 SOME RESULTS FOR SEMICIRCULAR AND POINTED ARCHES

The methods described in the foregoing have been applied to analyse the behaviour of semicircular and pointed masonry arches.

Starting with the stability area method, we shall limit ourselves to a brief illustration of the most meaningful aspects and results. Figure 5b shows the area of stability for the case of limit equilibrium for a semicircular arch with $\beta = 0°$ and $h = 50$ cm.

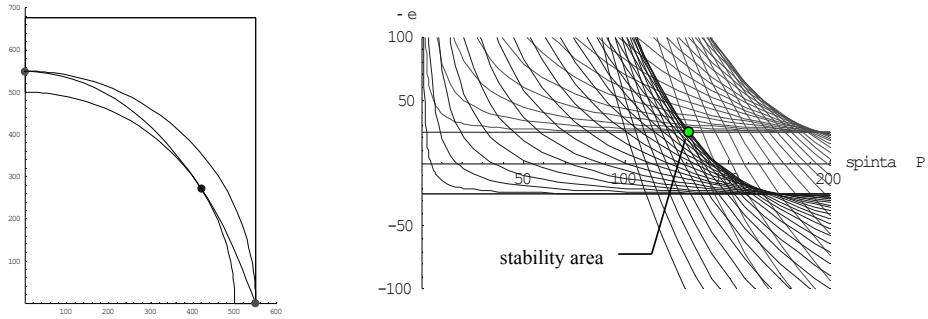

Figure 5 a, b. Line of thrust and stability area (semicircular arch; $\beta = 0°$, $h = 50$ cm).

The limit height of the wall compatible with the bearing capacity of the arch is reached when the area of stability shrinks to a point. In this case, the limit line of thrust is shown in Fig.5a.

By fixing the angle β and varying the cross-sectional thickness h, we find different values for the maximum height of the wall corresponding to a limit condition, as reported in the graphs below (figures 6 and 7), where the height of the wall is measured starting at the springings.

Figure 6 shows the corresponding results obtained for a semicircular and a pointed arch with $\beta = 0°$. It is interesting to observe that in this case, for small values of h, we find both a minimum and a maximum height corresponding to a limit equilibrium condition. Similar results are obtained for $\beta = 45°$ and $\beta = 60°$ (figure 7).

Figure 8a presents a plot of the maximum height of the wall against the thickness h for three different values of parameter β, namely $\beta = 0°$, 45° and 60°, for both circular and pointed arches. It is noteworthy that, almost for any h, *pointed arches allow for much greater wall heights than circular ones*. From an architectural point of view, it is also interesting to observe that such a result is in keeping with the greater slenderness of Gothic constructions.

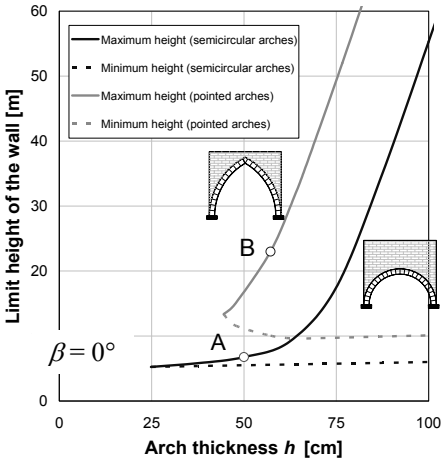

Figure 6. Limit height of the arch-wall system for a semicircular and a pointed arch ($\beta = 0°$).

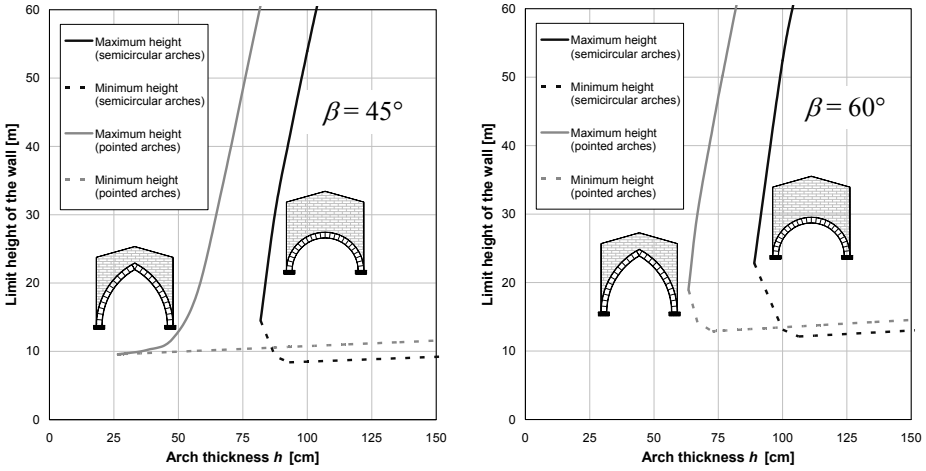

Figure 7. Limit height of the arch-wall system for a semicircular and a pointed arch (left: $\beta = 45°$; right: $\beta = 60°$).

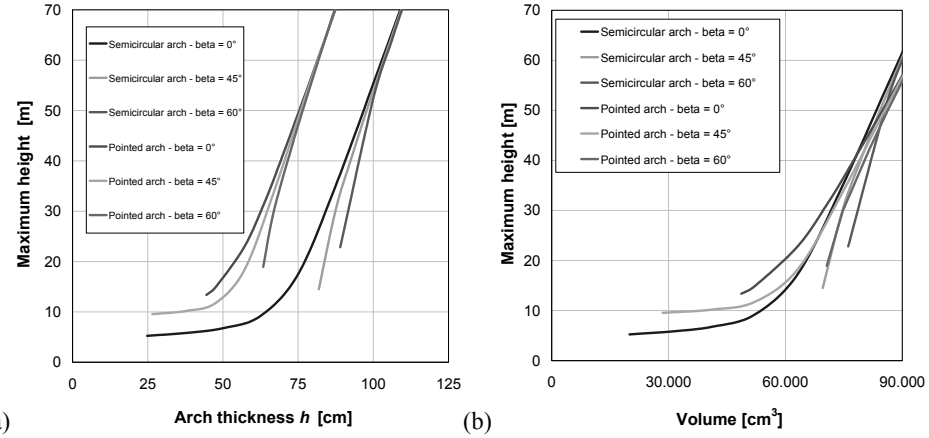

Figure 8. Maximum height of the arch-wall system versus arch thickness h (left) and versus volume of the arch (right).

As can be seen in figure 8, the minimum cross-sectional thickness compatible with equilibrium depends heavily on parameter β: for instance, min[h] is smaller for circular arches with $\beta = 0°$ than for pointed arches with $\beta = 45°$. Pointed arches consistently afford higher load capacities than semicircular arches of the same thickness h.

Another set of results regards the relation between the maximum wall height and the volume of the arch. This study offers an estimate of the volume of the *voussoirs*. As can be seen in figure 8b, the differences between semicircular and pointed arches are now considerably smaller, and parameter β influences the behaviour of the arch-wall system for small values of the volume. The semicircular arch with $\beta = 0°$ corresponds to the minimum volume compatible with the limit equilibrium: in this case, the extrados of the wall is tangent to that of the arch. For this volume value, circular arches with $\beta = 45°$, 60° and pointed arches with $\beta = 0°$, 45°, 60° would collapse. Increasing the volume, at first pointed arches with $\beta = 45°$, and then pointed arches with $\beta = 0°$ exhibit the best behaviour, reaching the maximum heights, while circular arches with $\beta = 45°$, 60° would still collapse. For greater values of the volume, instead, circular arches with $\beta = 45°$ attain the maximum height.

The values of the limit height of the wall obtained by applying the non-linear elastic model to the same loading cases illustrated above are in very good agreement with the corresponding values obtained via the stability area method, thus confirming the compatibility between the two methods. In addition, the non-linear elastic analysis enables following the evolution of the displacement and stress fields within the arch, as well as the extension of the non-linear regions as the load increases.

By way of example, figure 9 illustrates the deformed configuration and the distribution of non-linear regions for the circular arch already examined via the stability area method (point A in figure 6). The arch has radius R = 5.25 m, cross-sectional height h = 50 cm and it is loaded by its self-weight and the weight of a 6.75m-high wall. By reason of symmetry, only one half of the arch is shown in the figures.

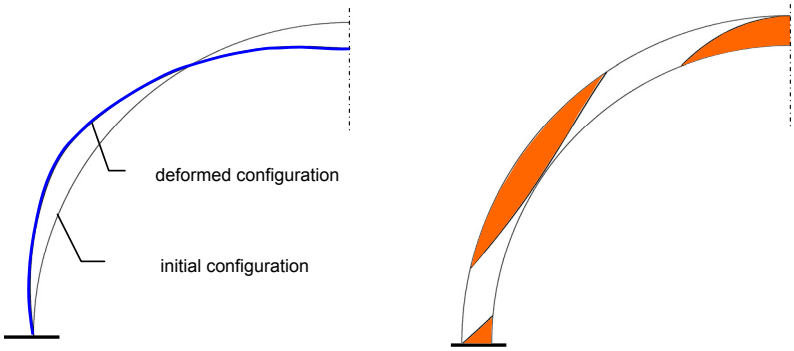

Figure 9. Left: deformed configuration (displacement magnified two times); right: non-linear regions under tension (in orange).

The height of the wall is very near the limit height as assessed by the stability area method (6.77 m) and is the highest value for which convergence of the numerical procedure is achieved. As is evident from the graph, the displacements in the neighbourhood of collapse are not at all negligible (the crown vertical displacement turns out to be about 21 cm). Moreover, wide zones along the arch are in a non-linear regime, thus leading to the supposition that widespread cracking would appear along the arch. The large increase in the magnitude of the displacements as the load approaches its limit value is also confirmed by the plot shown in figure 10.

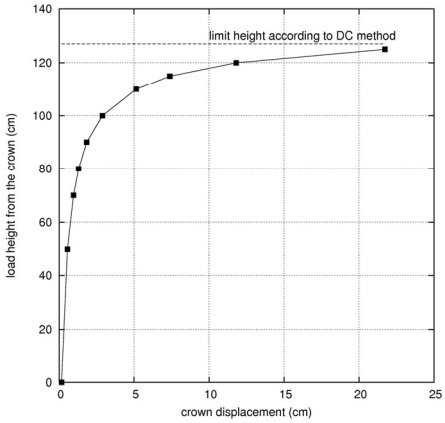

Figure 10. Plot of the crown vertical displacement for different values of the wall height.

Analogous results are obtained for pointed arches. The case of the pointed arch considered through the stability area method (point B in Figure 6) is illustrated below as an example. The arch has radius R = 10.57 m, cross-sectional height h = 57.2 cm. The numerical procedure con-

verged up to a wall height of 22.85 m (the stability area method yields a limit height of 23 m). Figure 11 shows the relative diagram of the extrados and intrados stresses, together with the distribution of the non-linear regions (green: in compression; orange: in tension). It should be observed that, in this case, the limit stress under compression is reached in some parts of the arch, and that the distribution of the non-linear regions is now slightly different from that found in the previous case of a circular arch, thus leading to the suspicion that in this case local crushing phenomena are likely to appear.

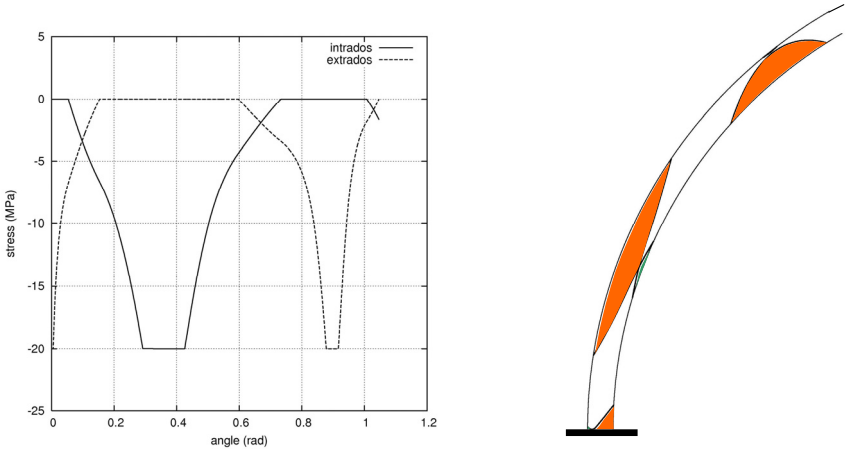

Figure 11. Extrados and intrados stresses (left)
and extension of the non-linear regions along the left half of the arch (right).

5 CONCLUSIONS

The load-bearing capacities of semicircular and pointed arches evaluated by means of the stability area method and non-linear elastic analysis turn out to be in very good agreement. The extension of the non-linear regions, as well as the magnitude of the displacements involved suggest that neglecting the effects of geometrical non-linearities in masonry structures could lead to dangerous overestimation of the actual value of the collapse load.

All the results confirm the common opinion according to which a pointed arch can bear a much higher wall than a semicircular arch of same span and cross-section, thereby allowing a greater slenderness of the whole structure.

REFERENCES

Aita, D., Barsotti, R., Bennati, S., Foce, F. 2004. The statics of pointed masonry arches between 'limit' and 'elastic' analysis. In P. Roca and E. Oñate (Eds), *Proc. Arch Bridges ARCH'04*, p. 353-362, Barcelona: CIMNE.

Alfano, G., Rosati, L., Valoroso, N. 2000. A numerical strategy for finite element analysis of no-tension materials. *Int. J. Numer. Meth. Engng*, 48, p. 317-350.

Bennati, S., Barsotti, R., 2001. Optimum radii of circular masonry arches. In C. Abdunur (ed.), *Proc. Third International Arch Bridges Conference – ARCH 01*, vol. 1, p. 489-498, Paris, France.

Bennati, S., Barsotti, R., 2007. A one-dimensional non linear elastic model for a masonry arch (forthcoming paper).

Foce F., Aita D., 2003. The masonry arch between limit and elastic analysis. A critical re-examination of Durand-Claye's method. In S. Huerta (ed.), *Proc. First Int. Congress on Construction History*, vol. II, p. 895-905. Madrid: Instituto Juan de Herrera.

Lourenço P.B., 2005. Assessment, diagnosis and strengthening of Outeiro Church, Portugal. *Construction and Building Materials*, 19, pp. 634–645.